

Liver-Specific Loss of Lipolysis-Stimulated Lipoprotein Receptor Triggers Systemic Hyperlipidemia in Mice

Prachiti Narvekar,¹ Mauricio Berriel Diaz,¹ Anja Kronen-Herzig,¹ Ulrike Hardeland,¹ Daniela Strzoda,¹ Sigrid Stöhr,² Marcus Frohme,³ and Stephan Herzig¹

OBJECTIVE—In mammals, proper storage and distribution of lipids in and between tissues is essential for the maintenance of energy homeostasis. In contrast, aberrantly high levels of triglycerides in the blood (“hypertriglyceridemia”) represent a hallmark of the metabolic syndrome and type 2 diabetes. As hypertriglyceridemia has been identified as an important risk factor for cardiovascular complications, in this study we aimed to identify molecular mechanisms in aberrant triglyceride elevation under these conditions.

RESEARCH DESIGN AND METHODS—To determine the importance of hepatic lipid handling for systemic dyslipidemia, we profiled the expression patterns of various hepatic lipid transporters and receptors under healthy and type 2 diabetic conditions. A differentially expressed lipoprotein receptor was functionally characterized by generating acute, liver-specific loss- and gain-of-function animal models.

RESULTS—We show that the hepatic expression of lipid transporter lipolysis-stimulated lipoprotein receptor (LSR) is specifically impaired in mouse models of obesity and type 2 diabetes and can be restored by leptin replacement. Experimental imitation of this pathophysiological situation by liver-specific knockdown of LSR promotes hypertriglyceridemia and elevated apolipoprotein (Apo)B and E serum levels in lean wild-type and ApoE knockout mice. In contrast, genetic restoration of LSR expression in obese animals to wild-type levels improves serum triglyceride levels and serum profiles in these mice.

CONCLUSIONS—The dysregulation of hepatic LSR under obese and diabetic conditions may provide a molecular rationale for systemic dyslipidemia in type 2 diabetes and the metabolic syndrome and represent a novel target for alternative treatment strategies in these patients. *Diabetes* 58:1040–1049, 2009

According to recent estimates, obesity-related type 2 diabetes will be diagnosed in 200–300 million people worldwide in 2010 (1). As part of the so-called metabolic syndrome, chronic hyperglycemia and dyslipidemia represent major causes for vascular complications in type 2 diabetic patients and result from defects in endocrine control systems that

From the ¹Emmy Noether and Marie Curie Research Group “Molecular Metabolic Control,” DKFZ-ZMBH Alliance, German Cancer Research Center Heidelberg, Heidelberg, Germany; the ²Department of Animal Physiology, Philipps University Marburg, Marburg, Germany; and the ³Technische universitat Braunschweig, Leibniz Institute for Applied Energy Conversion, Braunschweig, Germany.

Corresponding author: Stephan Herzig, s.herzig@dkfz.de.

Received 28 August 2008 and accepted 20 January 2009.

Published ahead of print at <http://diabetes.diabetesjournals.org> on 2 February 2009. DOI: 10.2337/db08-1184.

M.B.D. and A.K.-H. contributed equally to this work.

© 2009 by the American Diabetes Association. Readers may use this article as long as the work is properly cited, the use is educational and not for profit, and the work is not altered. See <http://creativecommons.org/licenses/by-nc-nd/3.0/> for details.

The costs of publication of this article were defrayed in part by the payment of page charges. This article must therefore be hereby marked “advertisement” in accordance with 18 U.S.C. Section 1734 solely to indicate this fact.

under normal conditions strictly balance glucose and lipid homeostasis within narrow limits (2).

Dyslipidemia, as associated with diabetic metabolism and the metabolic syndrome, is characterized by a so-called proatherogenic blood lipid profile, comprising low levels of HDLs, increased LDLs, and strongly increased levels of serum triglycerides associated with VLDLs. Indeed, hepatic VLDL release is increased in diabetes and is thought to drive other aspects of the dyslipidemia associated with this disorder (3). In fact, hypertriglyceridemia is considered to represent an important risk factor for atherosclerosis and subsequent cardiovascular complications in type 2 diabetic patients (4).

The regulation of plasma triglyceride levels is conferred through a complex interplay between different tissues and cell types (5). Dietary triglycerides within chylomicrons are hydrolyzed by adipose tissue and skeletal muscle lipoprotein lipase (LPL), effectively delivering free fatty acids to these peripheral tissues. The remaining particles, chylomicron remnants, are subsequently internalized by the liver. In addition to chylomicron-derived remnant particles, triglyceride-rich VLDLs are converted to remnants and returned to the liver. Although the ultimate fate of remnant particles has been clearly shown to be mediated by the liver (6), the identity and relative contribution of individual receptors involved in this process are still less clear. The LDL receptor (LDLR), the LDL receptor-related protein (LRP) 1, and scavenger receptor (SR)-B1 have been found to play only secondary roles in remnant clearance (7–11). Based on a series of biochemical studies and effects of whole-body heterozygosity in mice, Bihain and colleagues suggested that the lipolysis-stimulated receptor (LSR) serves as a remnant receptor (12–16).

Liver-selective insulin resistance was found to be sufficient to cause hypercholesterolemia and increase the susceptibility to atherosclerosis (17), suggesting a tight connection between endocrine control of hepatic metabolism and systemic lipid metabolism. It remains unclear to what extent endocrine circuits control hepatic lipoprotein receptor expression and/or function, thereby contributing to the observed dyslipidemia during obesity-related, insulin-resistant type 2 diabetes.

By profiling the expression of various lipid transporters in livers of healthy and diabetic mice under distinct nutritional conditions, in this study we discovered the dysregulation of LSR (15) in the liver as a common feature of various mouse models of obesity-related type 2 diabetes and demonstrated the importance of hepatic LSR action for the prevention of hypertriglyceridemia under physiological conditions.

RESEARCH DESIGN AND METHODS

Recombinant adenoviruses. An adenovirus expressing the LSR cDNA and a corresponding empty cytomegalovirus (CMV) control virus was cloned using

a modified pAd-BLOCK-iT vector system (Invitrogen, Karlsruhe, Germany). LSR cDNA was cloned by PCR standard procedures using primers directed against sequences deposited under GenBank accession number NM_017405. Adenoviruses expressing LSR-specific or nonspecific control oligonucleotides were produced using the BLOCK-iT Adenoviral RNAi expression system (Invitrogen) according to the manufacturer's instructions and purified by cesium chloride gradients (18).

Animal experiments. Male 8- to 12-week-old C57BKS, C57BL/6J, *db/db*, *ob/ob*, New Zealand black (NZB), New Zealand obese (NZO), and apolipoprotein (Apo)E knockout mice were obtained from Charles River Laboratories (Brussels, Belgium) and maintained on a 12-h light-dark cycle with unrestricted access to food. For starvation experiments, animals were fasted for 24 h with free access to water or fasted and refed for the remaining 6 h. For virus injections, 1×10^9 plaque-forming units per recombinant virus were administered via tail vein injection. In each experiment, seven animals received identical treatments. Mice were killed 7 days after adenovirus injection in the refed state. Insulin tolerance tests were performed as described previously (19). In high-fat diet experiments, C57BL6 mice were fed either a standard laboratory diet (10 energy percentage from fat, D12450B; Research Diets, New Brunswick, NJ) or a high-fat diet (45 energy percentage from fat, D12451; Research Diets) for 16 weeks (samples kindly provided by S. Kersten, Wageningen, Netherlands). Mice carrying a liver-specific knockout of the insulin receptor (LIRKO) have been described previously (19) (samples kindly provided by R. Kulkarni, Boston, MA). To deplete insulin-producing β -cells, C57BL/6J mice were treated with streptozotocin as described (20) (samples kindly provided by J.C. Brüning, Cologne, Germany). For leptin replacement studies, wild-type C57BL/6J and *ob/ob* mice were daily injected intraperitoneally with recombinant mouse leptin (5 μ g/g body weight) (R&D Systems, Wiesbaden, Germany) for 21 days. Organs including liver, epididymal fat pads, small intestine, and gastrocnemius muscles were collected after the corresponding time periods, weighed, snap-frozen, and used for further mRNA, protein, or metabolic analysis. Total body fat content was determined by a magnetic resonance imaging body composition analyzer (Echo Medical Systems, Houston, TX). All animal procedures have been approved by local authorities and are in accordance with National Institutes of Health guidelines.

Blood metabolites. Serum levels of glucose, triglycerides, cholesterol, ketone bodies, and free fatty acids were determined by using an automatic glucose monitor (One Touch, LifeScan) or commercial kits (Sigma, Munich, Germany; RANDOX, Crumlin, U.K.; WAKO, Neuss, Germany, respectively).

Hepatic VLDL release. VLDL production was determined after tyloxapol (Sigma) injection as described (21).

Lipid load tests. For an oral lipid load test, mice were fasted for 16 h and gavaged with 200 μ l olive oil. Alternatively, mice were fasted for 16 h, and 100 μ l of a 2.6% (v/v) intralipid emulsion in saline (Sigma) was administered intravenously. Serum samples were collected at various time points, and triglyceride levels were determined by commercial kits as above. Clearance was calculated by determining the area under the curves for each experimental group.

Fast protein liquid chromatography. Serum from seven mice per experimental group was pooled and subjected to fast protein liquid chromatography (FPLC) as described previously (22). Cholesterol and triglyceride levels were measured in the eluted fractions using commercial kits as above.

Tissue lipid extraction. Hepatic lipids were extracted as described previously (23), and triglyceride and total cholesterol contents were determined using commercial kits as above. Values were calculated as micromoles (triglycerides) or milligrams (cholesterol) per gram frozen tissue.

LPL activity. LPL activity measurements were performed as described (24) using frozen adipose tissue samples.

Quantitative TaqMan RT-PCR. Total RNA was extracted from homogenized mouse liver using the QIAzol reagent (Qiagen, Hilden, Germany) kit. cDNA was prepared by reverse transcription using oligo(dT) primer (Fermentas, St. Leon-Rot, Germany). cDNAs were amplified using assay-on-demand kits and an ABI PRISM 7700 Sequence detector (Applied Biosystems, Darmstadt, Germany). RNA expression data were normalized to levels of TATA box-binding protein RNA.

Protein analysis. Denatured SDS protein extracts from frozen liver homogenates or serum samples were loaded onto an 8% SDS-polyacrylamide gel, 4–12% gradient gels (Invitrogen), and blotted onto nitrocellulose membrane. Western blot assays were performed as described (25) using antibodies against valosin-containing protein (VCP) (Abcam, Cambridge, U.K.), ApoB, ApoE, or ApoAI (Santa Cruz, Heidelberg, Germany) or a mouse monoclonal antibody generated against the COOH-terminal fragment (amino acids 383–591) of murine LSR by standard procedures.

RNA interference. Oligonucleotides targeting mouse LSR (GenBank accession number NM_017405) (5'-GCACCTACCAGATGAGCAATA-3') were annealed and cloned into pENTR RNAi vector (Invitrogen). Nonspecific

oligonucleotides (5'-GATCTGATCGACACTGTAATG-3') with no significant homology to any mammalian gene sequence were used as nonsilencing controls in all experiments.

Cell culture. Primary mouse hepatocytes were isolated and cultured as described (26). Cells were treated with insulin (100 nmol/l) for 30 min to 24 h and harvested for mRNA expression analysis.

Statistical analysis. Statistical analyses were performed using a two-way ANOVA with Bonferroni-adjusted posttests or a *t* test in one-factorial designs, respectively. The significance level was at $P = 0.05$ or $P = 0.01$.

RESULTS

The importance of hepatic lipid handling for systemic lipidemia prompted us to profile the expression patterns of various lipid transporters/receptors under healthy and diabetic conditions. We analyzed cDNAs from wild-type C57BKS and *db/db* diabetic mice (27) under both fasted and refed conditions using quantitative real-time PCR. mRNA expression of fatty acid transporter CD36 and fatty acid transporter (FATP) 4 was induced in diabetic animals under refed and fasted or fasted conditions only, respectively, whereas FATP 5 was mildly elevated in diabetic mice in the refed state (Fig. 1A and B). Members of the ATP-binding cassette (ABC) cholesterol transporter family, ABCA1, ABCG1, and ABCG5 as well as bile salt export pump (BSEP), SR-BI (28), and FATP 3 showed no major differences in relative gene expression levels between healthy and diabetic conditions (Fig. 1A and B). ABCA1 and ABCG1 were found to be induced three- to fourfold by fasting under wild-type and diabetic conditions (Fig. 1A). Within the group of lipoprotein receptors, expression of LRP1 was not changed between fasting and refeeding or under diabetic conditions compared with wild-type controls, respectively (Fig. 1C). In contrast, mRNA expression of the LDLR was repressed in diabetic animals in the refed state (Fig. 1C). Furthermore, in the *db/db* diabetic state both fasting and refeeding LSR mRNA levels were substantially decreased compared with wild-type control animals (Fig. 1C), indicating that the loss of this hepatic receptor represents a specific feature of diabetic lipid metabolism. As no liver-specific loss or gain of function for LSR has been reported to date, these results prompted us to extend the analysis of LSR to additional models of type 2 diabetes and dyslipidemia. Consistent with results from *db/db* mice, hepatic LSR mRNA levels were diminished in *ob/ob* (29) as well as in NZO mice, the latter representing a multigenic model for type 2 diabetes (30), compared with corresponding controls (supplementary Fig. 1A and B, available in an online appendix at <http://care.diabetesjournals.org/cgi/content/full/db08-1184/DC1>), and tended to decrease upon feeding wild-type mice a high-fat diet (supplementary Fig. 1D, left). LSR mRNA levels in the small intestine, a second major tissue expressing this receptor (31), remained unaltered under all conditions (supplementary Fig. 1A and B). Importantly, the loss of hepatic LSR mRNA expression in diabetic and obese *db/db*, *ob/ob*, and NZO animals was confirmed at the protein level, as demonstrated by Western blot using a mouse monoclonal antibody against LSR (Fig. 1D, compare lanes 1–4 with lanes 5–8), whereas intestinal LSR protein levels were unchanged in these models (supplementary Fig. 1C).

Insulin plays an important role in hepatic lipid metabolism (32), suggesting that defective insulin signaling could be responsible for the inhibition of LSR expression in diabetic mice. LSR mRNA levels were not changed in mice carrying a liver-specific knockout of the insulin receptor (19) or in an insulin-deficient mouse model for type 1

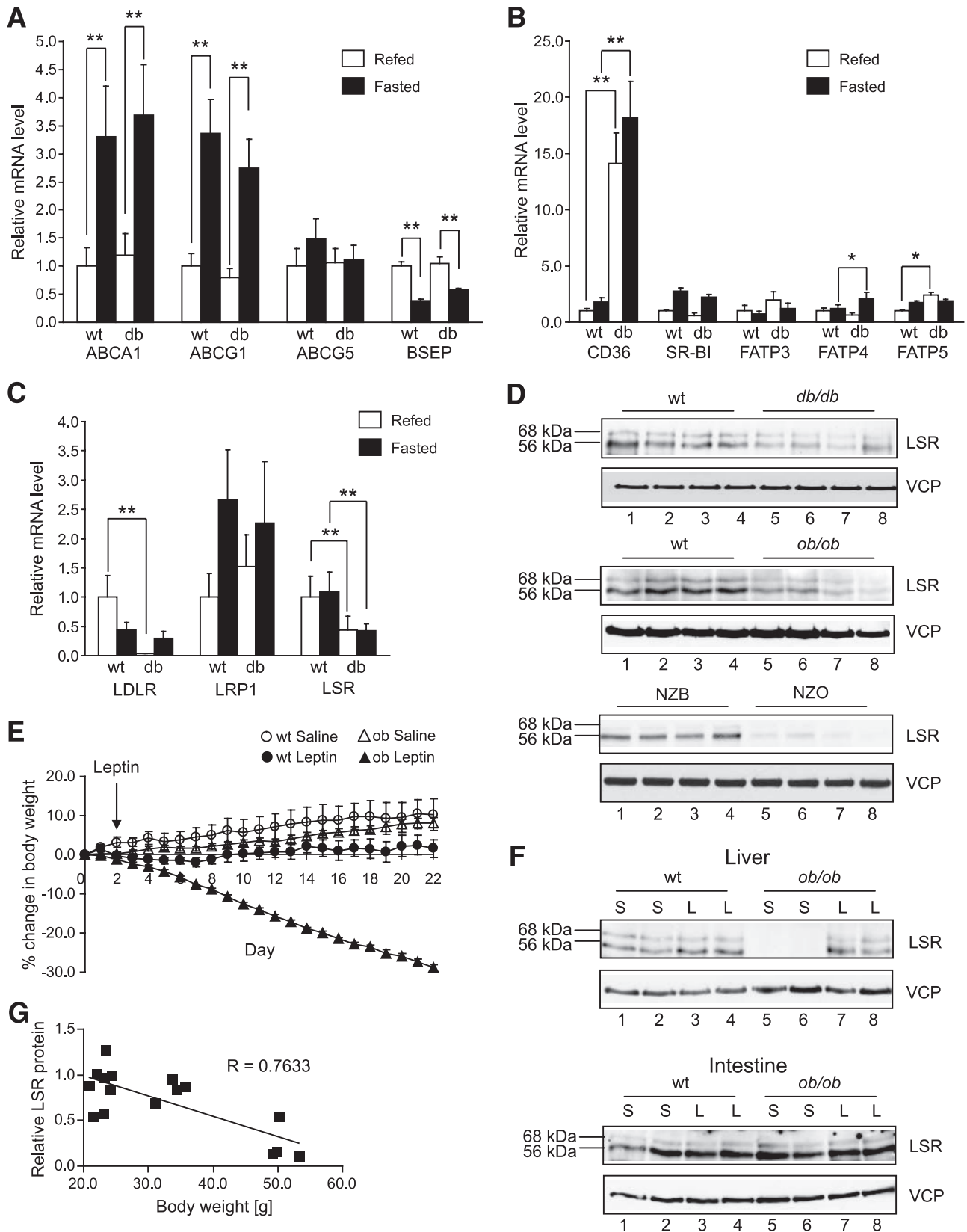


FIG. 1. Hepatic LSR expression is repressed in leptin-resistant type 2 diabetes. *A–C:* Quantitative PCR analysis of cholesterol/bile acid transporter (*A*), fatty acid transporter (*B*), and triglyceride/cholesterol transporter (*C*) mRNA levels in livers of C57BKS (wild-type [wt]) or *db/db* diabetic (*db*) mice under fasted (24 h) or refed (24 h fasted, 6 h refed) conditions as indicated ($n = 4$) (means \pm SE). $*P \leq 0.05$; $**P \leq 0.01$. *D:* Western blot of liver extracts from four representative wild-type or *db/db* (upper panel), *ob/ob* (middle panel), and NZB or NZO (lower panel) mice under refed conditions using LSR or VCP antibodies. *E:* Relative changes in body weight in wt and *ob/ob* mice treated daily with leptin (5 μ g/g body weight) for a period of 21 days (means \pm SE). *F:* Western blot of liver (upper panel) and intestinal (lower panel) extracts from the same mice as in *E* using LSR or VCP antibodies. Two representative animals per group are shown. *G:* Pearson correlation coefficient shown for relative hepatic LSR protein levels versus body weight in the same mice as in *E*. L, leptin; S, saline.

diabetes as compared to control littermates (supplementary Fig. 1D, *middle* and *right*), indicating that insulin per se is not responsible for the observed inhibition of LSR expression in the other models. Indeed, insulin treatment of primary mouse hepatocytes did not influence LSR mRNA expression in these cells (data not shown).

In addition to defective insulin signaling, obesity in mice and humans is characterized by leptin resistance (33,34). To test the hypothesis that leptin deficiency and/or resistance as exemplified by the *ob/ob* (29) or *db/db* (27) and NZO (35) models, respectively, are triggers for LSR inhibition under obese and diabetic conditions, we performed leptin replacement studies in *ob/ob* mice as a model for absolute leptin deficiency (29). Daily leptin administration over a 3-week period substantially reduced food intake (supplementary Fig. 1E), body weight (Fig. 1E), and whole-body fat content (supplementary Fig. 1F) in *ob/ob* mice. Remarkably, leptin replacement completely restored hepatic LSR protein expression in *ob/ob* animals to wild-type levels (Fig. 1F, *upper panel*, compare lanes 7–8 with lanes 1–2), but left intestinal LSR protein levels unaffected (Fig. 1F, *lower panel*). Hepatic LSR protein levels correlated significantly with body weight in both leptin- and saline-treated wild-type and *ob/ob* mice (Fig. 1G), suggesting that functional leptin signaling and action represent critical signals for the maintenance of hepatic LSR expression in lean, healthy animals. Together, these results indicate that the loss of hepatic LSR expression in turn represents a common feature of obesity-related, leptin-resistant type 2 diabetes.

To address the potential functional consequences of hepatic LSR inhibition for the pathophysiological phenotype in the above-described diabetes mouse models, we generated adenoviral constructs expressing LSR-specific or nonspecific small hairpin RNAs (shRNAs) and delivered these constructs into healthy, wild-type mice via tail vein injection. As shown in Fig. 2, LSR-specific shRNA delivery reduced hepatic LSR expression to 10% of control mRNA levels and almost completely eliminated hepatic LSR protein expression, as shown by Western blot analysis (Fig. 2A and B, *upper panel*). In contrast, no effect of the LSR shRNA adenovirus on LSR mRNA and protein expression levels in adipose tissue, skeletal muscle, or small intestine could be observed (Fig. 2A and B, *lower panel*). These experiments validated the previously reported liver specificity of this gene delivery technology (25) and allowed the exploration of liver-specific LSR functions for systemic metabolism in the absence of potentially confounding effects of LSR ablation in other tissues, as reported recently (16). Importantly, LSR shRNA adenovirus did not affect the mRNA and/or protein expression of related lipoprotein receptors, LDLR, LRP1, and SR-B1 (Fig. 2C and supplementary Fig. 2A), thereby excluding compensatory effects of these receptors in response to acute LSR gene knockdown.

Phenotypic analysis of liver-specific LSR knockdown animals demonstrated that the loss of hepatic LSR resulted in an almost threefold induction of serum triglyceride levels compared with control littermates and significantly elevated serum total cholesterol already 7 days after adenovirus delivery (Fig. 2D). In contrast, hepatic triglyceride stores were found to be lowered by 75% upon hepatic LSR knockdown, and hepatic cholesterol content was also significantly diminished (Fig. 2D). Importantly, these effects of LSR knockdown were only observed in the refed state—not under fasting conditions (supplementary Fig.

2B), suggesting that LSR specifically affects postprandial lipid homeostasis. LSR deficiency had no effect on systemic insulin sensitivity as determined by an insulin tolerance test (supplementary Fig. 2C). In addition, body weight (supplementary Fig. 2D), serum glucose (supplementary Fig. 2E), free fatty acids (FFAs) (supplementary Fig. 2F), total serum ketone body levels (supplementary Fig. 2G), whole-body fat content (supplementary Fig. 2H), and adipose tissue LPL activity (supplementary Fig. 2I) remained unchanged, showing that hepatic LSR deficiency specifically determines hepatic and systemic triglyceride handling. Indeed, liver-specific LSR knockdown significantly delayed systemic triglyceride clearance in an intravenous lipid load test and also tended to delay clearance of an oral lipid load (Fig. 2E and F). In contrast, analysis of hepatic VLDL secretion rates demonstrated that LSR-specific shRNA treatment had no effect on liver VLDL output compared with that of control littermates (supplementary Fig. 2J), further supporting the notion that hepatic LSR activity is particularly involved in the clearance and uptake of circulating serum triglycerides.

We next sought to explore the basis for the observed hypertriglyceridemia in liver-specific LSR knockdown animals in more detail. To this end, we performed FPLC analysis of serum samples from LSR knockdown and control littermates. Consistent with the induction of total serum triglyceride levels, LSR deficiency promoted a significant increase in triglycerides associated with the VLDL/chylomicron and LDL fractions (Fig. 3A). In addition, LSR shRNA treatment caused an increase in VLDL/chylomicron and HDL cholesterol content compared with control shRNA-treated littermates (Fig. 3B). In accordance with these profiles, the levels of ApoB and ApoE, the major lipoproteins of VLDL, intermediate-density lipoproteins, and chylomicrons were increased in serum of liver-specific LSR knockdown mice compared with controls, whereas ApoAI remained unchanged (Fig. 3C). Thus, liver-specific LSR deficiency produced hypertriglyceridemia with triglyceride-enriched VLDL particles and elevated ApoB/E serum levels as commonly associated with type 2 diabetes and the metabolic syndrome.

We aimed to explore the relative importance of ApoB and ApoE particles for the LSR-mediated effects on systemic triglyceride levels. To this end, we used ApoE knockout mice (*ApoE*^{-/-}) as a standard model for systemic dyslipidemia and total ApoE deficiency (36). Adenoviral LSR shRNA delivery efficiently inhibited both mRNA and protein expression of LSR in livers of *ApoE*^{-/-} mice (Fig. 4A and B), but left intestinal LSR expression levels unaffected (Fig. 4A). As shown for wild-type mice before (Fig. 2), hepatic knockdown of LSR increased total serum triglyceride levels in *ApoE*^{-/-} mice by twofold (Fig. 4C) and lowered hepatic triglyceride stores in these animals (Fig. 4C). Indeed, FPLC analysis revealed a substantial increase in the VLDL-related serum triglyceride fraction upon LSR knockdown in *ApoE*^{-/-} mice (Fig. 4D), indicating that LSR exerts its regulatory impact on circulating triglycerides mainly through the interaction with ApoB with secondary rises in ApoE in response to hepatic LSR deficiency in wild-type mice (Fig. 2). Consistent with a specific effect of LSR on triglyceride metabolism, loss of hepatic LSR expression produced no effects on body weight (supplementary Fig. 3A), serum glucose (supplementary Fig. 3B), FFAs (supplementary Fig. 3C), and total ketone body levels (supplementary Fig. 3D). In addition, LSR knockdown in *ApoE*^{-/-} mice slightly influenced se-

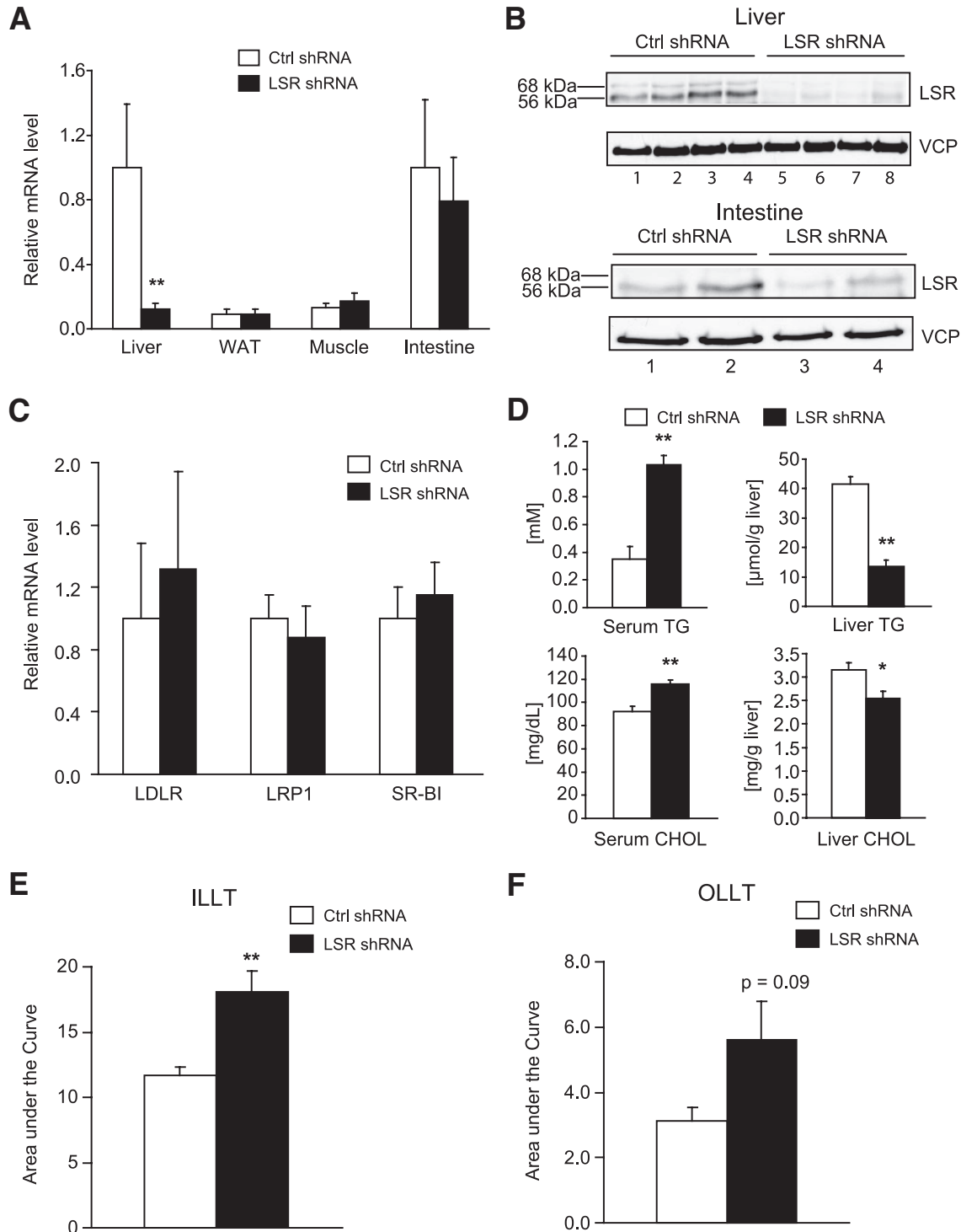


FIG. 2. Liver-specific loss of LSR promotes hypertriglyceridemia. **A:** Quantitative PCR analysis of LSR mRNA levels in livers, white adipose tissue (WAT), skeletal muscle, and small intestine of C57BL/6J mice injected with control or LSR-specific shRNA adenovirus at day 7 after virus delivery ($n = 7$). **B:** Western blot of liver (*upper panel*) and intestinal (*lower panel*) extracts from four and two representative control (Ctrl) or LSR shRNA-injected C57BL/6J mice using LSR or VCP antibodies at day 7 after virus delivery. **C:** Quantitative PCR analysis of LDLR, LRP1, and SR-B1 mRNA levels in livers of the same mice as in **A** ($n = 7$). **D:** Serum and liver triglyceride (TG) and cholesterol (CHOL) levels in the same mice as in **A** ($n = 7$). Values are shown for the refed state. **E:** Intravenous lipid load test (ILLT) in the same mice as in **A**. Mice were injected intravenously with 100 μ l of a 2.6% lipid emulsion and serum triglyceride levels were followed for 2 h. Average area under the curve (arbitrary units) is shown ($n = 7$) (means \pm SE). **F:** Oral lipid load test (OLLT) in the same mice as in **A**. Mice received an oral load of 200 μ l olive oil and serum triglyceride levels were followed for 6 h. Average area under the curve (arbitrary units) is shown ($n = 7$) (means \pm SE).

rum cholesterol (supplementary Fig. 3E) but had no effect on liver cholesterol levels (supplementary Fig. 3F) or on apolipoprotein-associated cholesterol serum profiles as determined by FPLC analysis (supplementary Fig. 3G).

These results favored the hypothesis that LSR-dependent ApoB clearance from the circulation counteracts hypertriglyceridemic dyslipidemia in ApoE^{-/-} mice. To verify this assumption independently, we used an adeno-

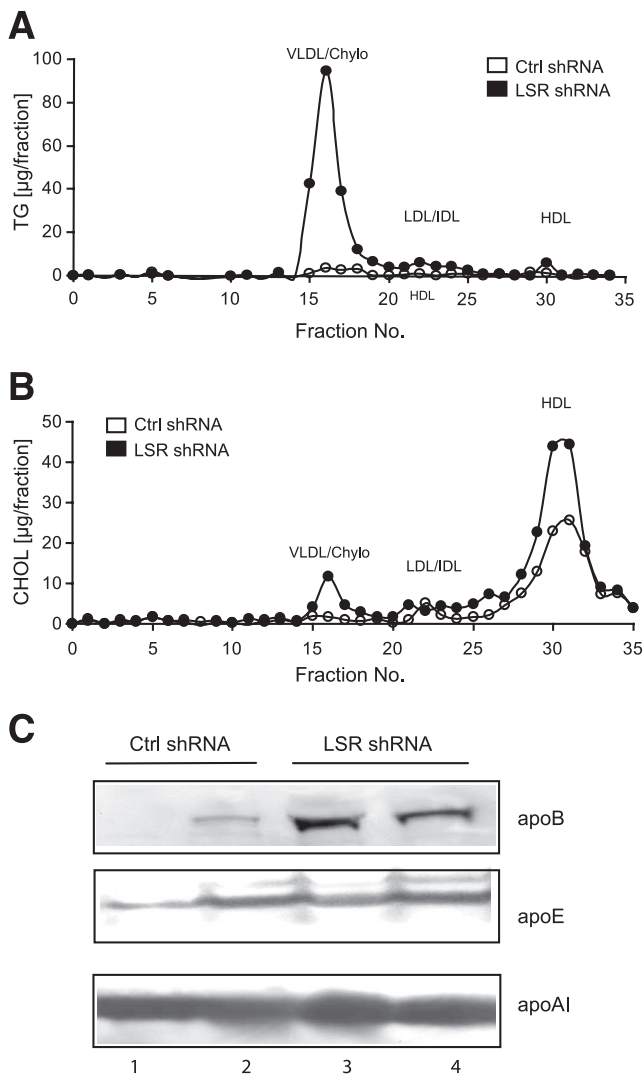


FIG. 3. Hepatic LSR deficiency specifically affects VLDL triglyceride (TG) and ApoB/E levels. **A:** Triglyceride content of serum fractions from control (Ctrl) or LSR shRNA-injected C57BL/6J mice at day 7 after injection. Serum pools of $n = 7$ animals per group were separated by FPLC. Individual fraction numbers are indicated. **B:** Cholesterol (CHOL) content of serum fractions from the same mice as in **A**. **C:** Western blot of serum samples from two representative control or LSR shRNA-injected C57BL/6J mice using ApoB, ApoE, or ApoAI antibodies at day 7 after virus delivery. Chylo, chylomicrons; IDL, intermediate-density lipoprotein.

virus carrying the LSR cDNA to specifically overexpress LSR in livers of wild-type or ApoE^{-/-} animals (Fig. 4E and supplementary Fig. 4A). To this end, LSR adenovirus left intestinal LSR mRNA and protein levels unaffected (Fig. 4E and supplementary Fig. 4B). In agreement with previous results (Fig. 2), LSR overexpression did not influence body weight (supplementary Fig. 4C), serum glucose (supplementary Fig. 4D), FFAs (supplementary Fig. 4E), total ketone body levels (supplementary Fig. 4F), or total serum or liver cholesterol levels and/or serum distribution (supplementary Fig. 4G–I). However, hepatic LSR overexpression significantly decreased serum triglyceride levels in ApoE^{-/-} mice (Fig. 4F) and substantially reduced VLDL-associated triglycerides in hyperlipidemic ApoE^{-/-} animals (Fig. 4G), substantiating the conclusion that LSR counteracts systemic hypertriglyceridemia via the induction of ApoB-dependent triglyceride clearance from the circulation.

Thus far, the data demonstrated that the hepatic triglyceride receptor LSR represents a critical checkpoint for systemic triglyceride metabolism and that the absence of LSR in the liver promotes a hypertriglyceridemic shift toward triglyceride-rich, ApoB/ApoE-containing lipoproteins in lean mice. The downregulation of LSR in animals with obesity-related, leptin-resistant type 2 diabetes (Fig. 1) suggested that the reduction of LSR expression might contribute to the pathophysiological phenotype of these animals and promote aberrant triglyceride metabolism under these conditions.

To finally test this hypothesis, we delivered the LSR overexpression adenovirus into *ob/ob* mice (29). Adenoviral gene delivery restored hepatic expression of LSR in *ob/ob* mice to physiological wild-type amounts at mRNA (Fig. 5A) and protein (Fig. 5B) levels. At day 7 after virus injection, LSR reconstitution in *ob/ob* mice had no effects on body weight (supplementary Fig. 5A), serum glucose (supplementary Fig. 5B), FFAs (supplementary Fig. 5C), and total body fat content (supplementary Fig. 5D) compared with control-injected littermates. LSR restoration in *ob/ob* livers triggered a significant reduction in serum triglyceride and cholesterol levels (Fig. 5C), again demonstrating the specificity of LSR action for hepatic and systemic lipid metabolism even under obese conditions. To this end, genetic LSR reconstitution in *ob/ob* mice reduced VLDL/chylomicron and LDL triglyceride levels, while simultaneously decreasing circulating LDL/HDL1 (37) and HDL cholesterol levels in these animals (Fig. 5D). Interestingly, hepatic triglyceride and cholesterol content remained unchanged in response to LSR overexpression (Fig. 5C), suggesting intrahepatic compensation for increased triglyceride uptake. Indeed, correlating with significantly increased serum ketone body levels (supplementary Fig. 5E), mRNA levels of genes in the fatty acid oxidation pathway but not in the lipogenic program were found to be induced in LSR-overexpressing *ob/ob* mice (supplementary Fig. 5G and H), which was further associated with an increase in hepatic VLDL release (supplementary Fig. 5F).

Together, these data indicate that the lipid receptor (LSR) represents a key checkpoint in hepatic and systemic triglyceride metabolism. The downregulation of LSR during the manifestation of leptin-resistant, obesity-related type 2 diabetes may contribute to the commonly observed hypertriglyceridemia in diabetic and obese subjects and may further aggravate the risk for cardiovascular complications under these conditions.

DISCUSSION

Detailed molecular mechanisms in the pathogenesis of clinically severe aberrations in circulating lipid levels as associated with obesity and type 2 diabetes have not been completely defined. We identify an unexpected loss of function of the remnant lipoprotein receptor (LSR) as a common feature of obesity-related type 2 diabetic conditions in mouse models.

LSR has been initially found to be involved in the degradation of LDL in fibroblasts from a subject homozygous for familial hypercholesterolemia and lacking the LDLR (38). Genetic inactivation of the LSR gene leads to embryonic lethality (31), and studies on phenotypic consequences of whole-body LSR heterozygosity demonstrated effects on systemic triglyceride metabolism (16). Although extrahepatic functions of LSR remain unclear,

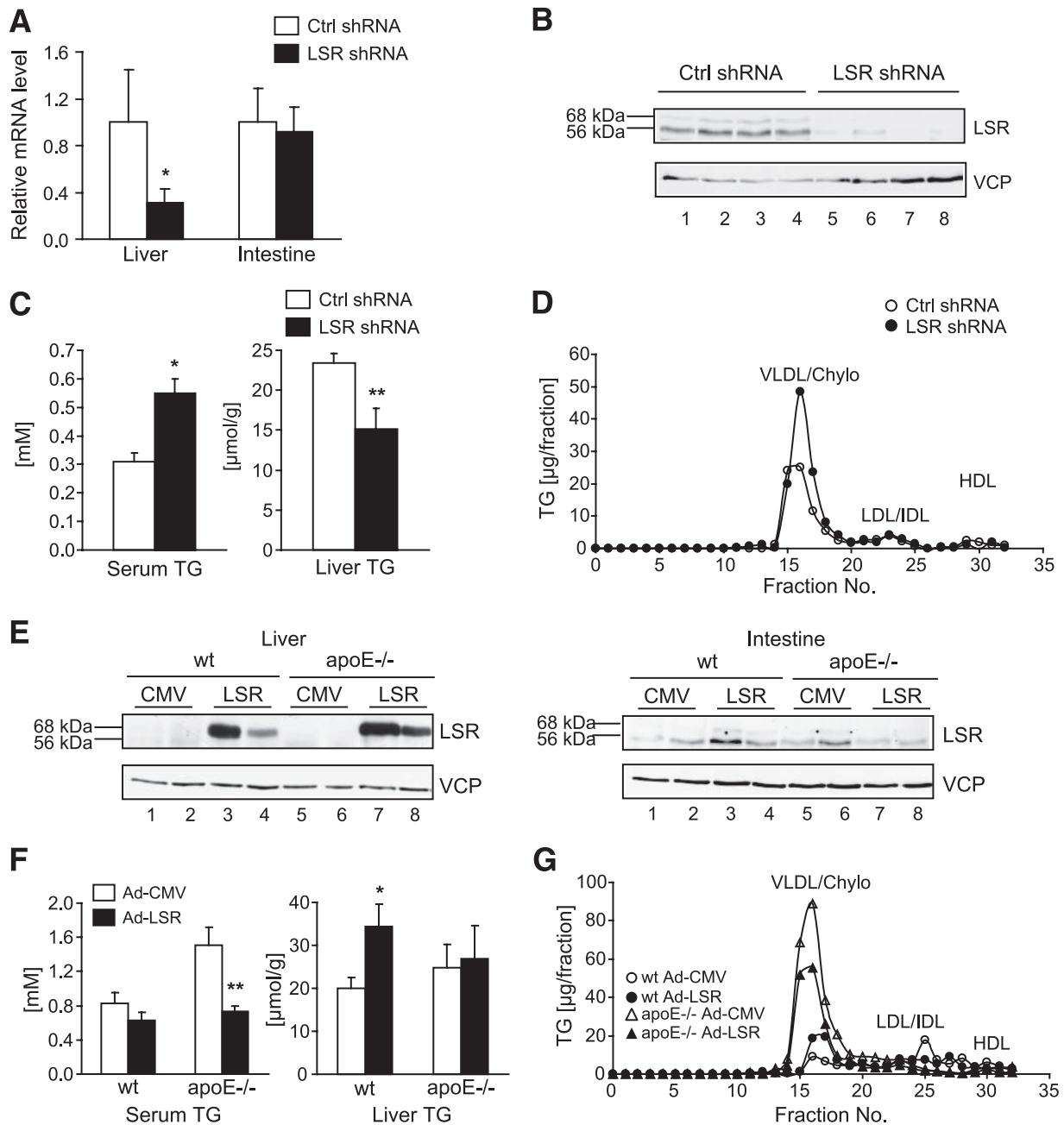


FIG. 4. Hepatic LSR controls triglyceride (TG) levels in ApoE^{-/-} mice. **A:** Quantitative PCR analysis of LSR mRNA levels in livers and small intestine of ApoE^{-/-} mice injected with control (Ctrl) or LSR-specific shRNA adenovirus at day 7 after virus delivery ($n = 7$) (means \pm SE). ** $P \leq 0.01$. **B:** Western blot of liver extracts from four representative control or LSR shRNA-injected ApoE^{-/-} mice using LSR or VCP antibodies at day 7 after virus delivery. **C:** Serum and liver triglyceride levels in the same mice as in **A** ($n = 7$) (means \pm SE). * $P \leq 0.05$; ** $P \leq 0.01$. **D:** Triglyceride content of serum fractions from control or LSR shRNA-injected ApoE^{-/-} mice at day 7 after injection. Serum pools of $n = 7$ animals per group were separated by FPLC. Individual fraction numbers indicated. Chylo, chylomicrons; IDL, intermediate-density lipoprotein. **E:** Western blot of liver (*upper panel*) and intestinal (*lower panel*) extracts from two representative wild-type (wt) and ApoE knockout (ApoE^{-/-}) mice injected with control (Ad-CMV) or LSR overexpression (Ad-LSR) adenovirus, respectively, using LSR or VCP antibodies at day 7 after virus delivery. **F:** Serum and liver triglyceride levels in the same mice as in **E** ($n = 7$) (means \pm SE). * $P \leq 0.05$; ** $P \leq 0.01$. **G:** Triglyceride content of serum fractions from the same mice as in **E**. Serum pools of $n = 7$ animals per group were separated by FPLC. Individual fraction numbers are indicated.

our studies provide the first evidence for a tissue-specific function of LSR in the liver. Our functional analysis of liver-specific LSR deficiency suggests that LSR plays a critical role in the clearance of triglyceride-rich, ApoB-containing VLDL particles, especially in the postprandial phase (Fig. 2), as loss of LSR function in both wild-type and ApoE^{-/-} mice promoted the occurrence of an aberrant lipid profile with high serum triglyceride and ApoB/ApoE levels (Figs. 2 and 3). The fact that our liver-specific LSR knockdown displayed a more severe

triglyceride phenotype than the hypertriglyceridemia in LSR heterozygous mice (16) indicates that the liver indeed represents the major site of LSR action. This is supported by the absence of changes in intestinal LSR expression levels in diabetes models (Fig. 1) as well as by the liver LSR-dependent clearance of intravenous lipid challenges (Fig. 2F). In line with these in vivo data, cellular studies in isolated hepatocytes have shown an important role of LSR in ApoB/E-containing lipoprotein uptake in vitro (12,16,39), its high affinity for triglyceride-rich lipopro-

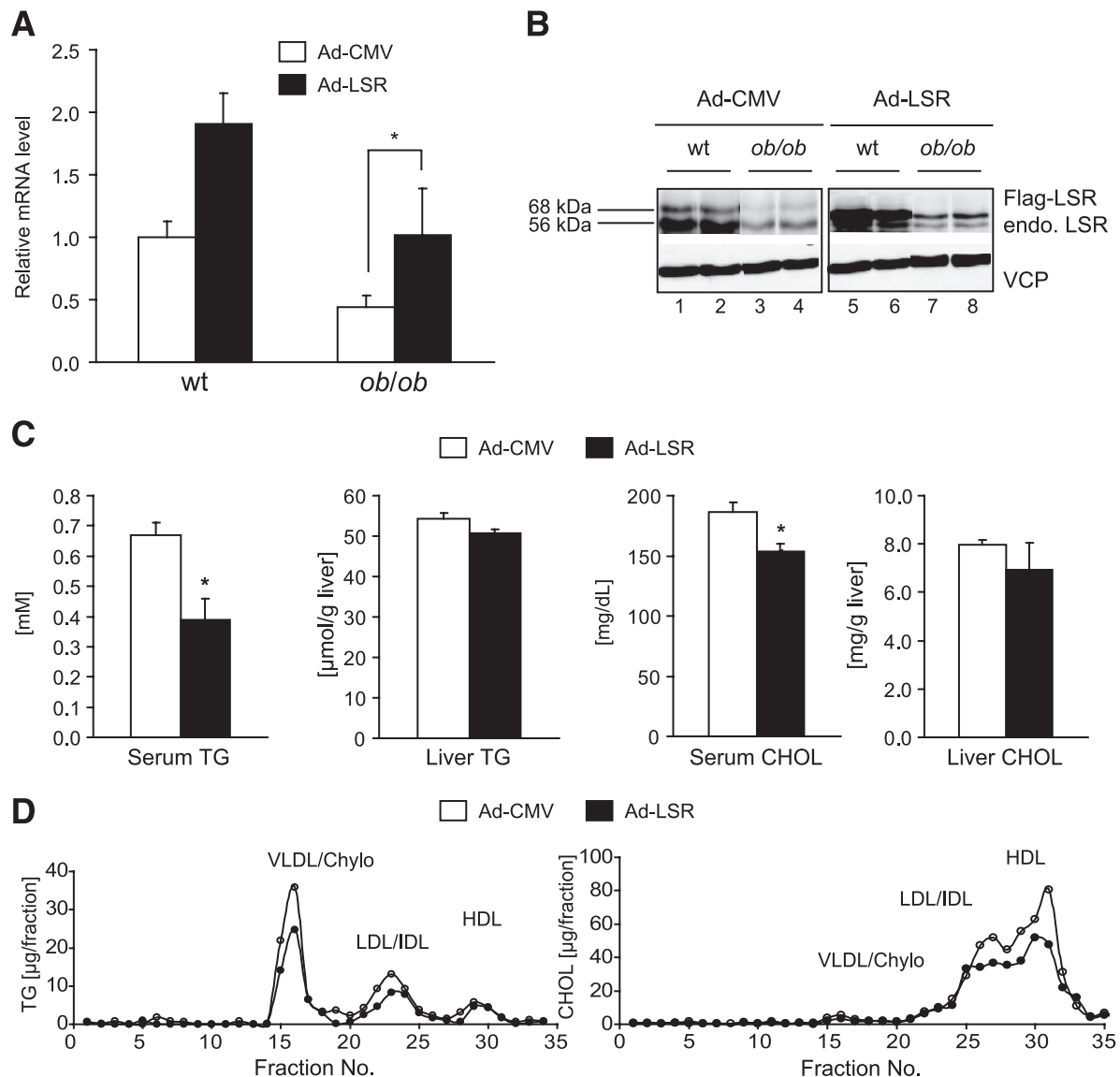


FIG. 5. Hepatic LSR restoration lowers serum triglyceride (TG) in obese mice. **A:** Quantitative PCR analysis of LSR mRNA levels in livers of C57BL/6J and *ob/ob* mice injected with control (Ad-CMV) or LSR-expressing (Ad-LSR) adenovirus at day 7 after virus delivery ($n = 7$) (means \pm SE). $*P \leq 0.05$. **B:** Western blot of liver extracts from two representative control (Ad-CMV) or LSR-expressing (Ad-LSR) adenovirus-injected C57BL/6J and *ob/ob* mice using LSR or VCP antibodies at day 7 after virus delivery. Labels indicate Flag-tagged LSR expression by adenovirus delivery, comigrating with the endogenous 68-kDa LSR subunit, and endogenous LSR levels representing the 56-kDa subunit in mice receiving control virus. **C:** Serum and liver triglyceride and cholesterol (CHOL) levels in *ob/ob* mice as in **A** and **B**, injected with control (Ad-CMV) or LSR-expressing (Ad-LSR) adenovirus ($n = 7$) (means \pm SE). $*P \leq 0.05$. **D:** Triglyceride (*upper panel*) and cholesterol (*lower panel*) content of serum fractions from the same mice as in **C**. Serum pools of $n = 7$ animals per group were separated by FPLC. Individual fraction numbers are indicated. Chylo, chylomicrons.

teins, and its inhibition by ApoCIII (15). It is tempting to speculate that the observed hypertriglyceridemia in ApoCIII transgenic mice (at least in part) can be explained by its inhibitory effect on LSR function (40).

In addition to ApoB-containing remnant clearance, elevated HDL cholesterol along with unaltered ApoAI (Fig. 2G and H) levels and significantly reduced HDL cholesterol in LSR-overexpressing *ob/ob* mice (Fig. 5D) imply a role of LSR also in the clearance of HDL cholesterol. Indeed, similar effects have been observed in mice deficient in the HDL receptor, SR-BI (28), and overexpression of SR-BI results in reduced plasma concentrations of HDL cholesterol (41). Whether the mechanisms of clearance of triglyceride-rich lipoproteins and a potential role of LSR in reverse cholesterol uptake are regulated by a common upstream signal needs to be further investigated.

This study provides evidence for a unique and specific role of hepatic LSR in systemic lipid homeostasis. Our pharmacological and genetic reconstitution studies demonstrate that liver-specific restoration of LSR is sufficient to improve VLDL triglyceride levels in obese and ApoE^{-/-} mice, promoting the notion that the inhibition of LSR expression in liver represents a critical determinant of pathophysiological lipid homeostasis in obesity-related type 2 diabetes. Indeed, leptin resistance as frequently observed under these conditions (33,34) seems to provide the endocrine explanation for the downregulation of LSR during obesity and/or weight gain (Fig. 1F–H) as long-term restoration of functional leptin signaling is sufficient to maintain hepatic LSR levels, thereby correlating with improved body weight (Fig. 1G). Further studies will be necessary to clarify the role of LSR as a molecular

checkpoint for long-term complications of dyslipidemia, such as cardiovascular damage and atherosclerosis. In this regard, the development of compounds that specifically modulate LSR function in the liver may provide useful adjunct antidyslipidemic therapy for patients with obesity and type 2 diabetes.

ACKNOWLEDGMENTS

This work was supported by a grant from the Deutsche Forschungsgemeinschaft (He3260/2-1) and a Marie Curie Excellence Grant (European Commission) to S.H.

No potential conflicts of interest relevant to this article were reported.

We thank Tobias Dick, Susanne Heck, Allan Jones, Philipp Kulozik, Dagmar Metzger, Lars Weingarten, Hanswalter Zentgraf, and Anja Ziegler for experimental advice and technical support and J.C. Brüning (Cologne, Germany), S. Kersten (Wageningen, the Netherlands), and R. Kulkarni (Boston, MA) for providing reagents.

REFERENCES

- Amos AF, McCarty DJ, Zimmet P. The rising global burden of diabetes and its complications: estimates and projections to the year 2010. *Diabet Med* 1997;14(Suppl. 5):S1-S85
- Brownlee M. Biochemistry and molecular cell biology of diabetic complications. *Nature* 2001;414:813-820
- Chahil TJ, Ginsberg HN. Diabetic dyslipidemia. *Endocrinol Metab Clin North Am* 2006;35:491-510, vii-viii
- Ginsberg HN. Diabetic dyslipidemia: basic mechanisms underlying the common hypertriglyceridemia and low HDL cholesterol levels. *Diabetes* 1996;45(Suppl. 3):S27-S30
- Duval C, Muller M, Kersten S. PPAR α and dyslipidemia. *Biochim Biophys Acta* 2007;1771:961-971
- Havel RJ. Chylomicron remnants: hepatic receptors and metabolism. *Curr Opin Lipidol* 1995;6:312-316
- Herz J, Hamann U, Rogne S, Myklebost O, Gausepohl H, Stanley KK. Surface location and high affinity for calcium of a 500-kd liver membrane protein closely related to the LDL-receptor suggest a physiological role as lipoprotein receptor. *EMBO J* 1988;7:4119-4127
- Rohlmann A, Gotthardt M, Hammer RE, Herz J. Inducible inactivation of hepatic LRP gene by cre-mediated recombination confirms role of LRP in clearance of chylomicron remnants. *J Clin Invest* 1998;101:689-695
- Herz J, Qiu SQ, Oesterle A, DeSilva HV, Shafi S, Havel RJ. Initial hepatic removal of chylomicron remnants is unaffected but endocytosis is delayed in mice lacking the low density lipoprotein receptor. *Proc Natl Acad Sci USA* 1995;92:4611-4615
- Ishibashi S, Brown MS, Goldstein JL, Gerard RD, Hammer RE, Herz J. Hypercholesterolemia in low density lipoprotein receptor knockout mice and its reversal by adenovirus-mediated gene delivery. *J Clin Invest* 1993;92:883-893
- Out R, Hoekstra M, de Jager SC, de Vos P, van der Westhuyzen DR, Webb NR, Van Eck M, Biessen EA, Van Berkel TJ. Adenovirus-mediated hepatic overexpression of scavenger receptor class B type I accelerates chylomicron metabolism in C57BL/6J mice. *J Lipid Res* 2005;46:1172-1181, 2005
- Mann CJ, Khallou J, Chevreuril O, Troussard AA, Guermani LM, Launay K, Delplanque B, Yen FT, Bihain BE. Mechanism of activation and functional significance of the lipolysis-stimulated receptor: evidence for a role as chylomicron remnant receptor. *Biochemistry* 1995;34:10421-10431
- Mann CJ, Troussard AA, Yen FT, Hannouche N, Najib J, Fruchart JC, Lotteau V, Andre P, Bihain BE. Inhibitory effects of specific apolipoprotein C-III isoforms on the binding of triglyceride-rich lipoproteins to the lipolysis-stimulated receptor. *J Biol Chem* 1997;272:31348-31354
- Troussard AA, Khallou J, Mann CJ, Andre P, Strickland DK, Bihain BE, Yen FT. Inhibitory effect on the lipolysis-stimulated receptor of the 39-kDa receptor-associated protein. *J Biol Chem* 1995;270:17068-17071
- Yen FT, Masson M, Clossais-Besnard N, Andre P, Grosset JM, Bougueleret L, Dumas JB, Guerassimenko O, Bihain BE. Molecular cloning of a lipolysis-stimulated remnant receptor expressed in the liver. *J Biol Chem* 1999;274:13390-13398
- Yen FT, Roitel O, Bonnard L, Notet V, Pratte D, Stenger C, Magueur E, Bihain BE. Lipolysis stimulated lipoprotein receptor: a novel molecular link between hyperlipidemia, weight gain and atherosclerosis in mice. *J Biol Chem* 2008;283:25650-25659
- Biddinger SB, Hernandez-Ono A, Rask-Madsen C, Haas JT, Aleman JO, Suzuki R, Scapa EF, Agarwal C, Carey MC, Stephanopoulos G, Cohen DE, King GL, Ginsberg HN, Kahn CR. Hepatic insulin resistance is sufficient to produce dyslipidemia and susceptibility to atherosclerosis. *Cell Metab* 2008;7:125-134
- Becker TC, Noel RJ, Coats WS, Gomez-Foix AM, Alam T, Gerard RD, Newgard CB. Use of recombinant adenovirus for metabolic engineering of mammalian cells. *Methods Cell Biol* 1994;43(Pt. A):161-189
- Michael MD, Kulkarni RN, Postic C, Previs SF, Shulman GI, Magnuson MA, Kahn CR. Loss of insulin signaling in hepatocytes leads to severe insulin resistance and progressive hepatic dysfunction. *Mol Cell* 2000;6:87-97
- Dhahbi JM, Mote PL, Cao SX, Spindler SR. Hepatic gene expression profiling of streptozotocin-induced diabetes. *Diabetes Technol Ther* 2003;5:411-420
- Mandard S, Zandbergen F, van Straten E, Wahli W, Kuipers F, Muller M, Kersten S. The fasting-induced adipose factor/angiopoietin-like protein 4 is physically associated with lipoproteins and governs plasma lipid levels and adiposity. *J Biol Chem* 2006;281:934-944
- Lichtenstein L, Berbee JF, van Dijk SJ, van Dijk KW, Bensadoun A, Kema IP, Voshol PJ, Muller M, Rensen PC, Kersten S. Angptl4 upregulates cholesterol synthesis in liver via inhibition of LPL- and HL-dependent hepatic cholesterol uptake. *Arterioscler Thromb Vasc Biol* 2007;27:2420-2427
- Lee Y, Wang MY, Kakuma T, Wang ZW, Babcock E, McCorkle K, Higa M, Zhou YT, Unger RH. Liporegulation in diet-induced obesity: the anti-steatotic role of hyperleptinemia. *J Biol Chem* 2001;276:5629-5635
- Klingenspor M, Klaus S, Wiesinger H, Heldmaier G. Short photoperiod and cold activate brown fat lipoprotein lipase in the Djungarian hamster. *Am J Physiol* 1989;257:R1123-R1127
- Herzig S, Long F, Jhala US, Hedrick S, Quinn R, Bauer A, Rudolph D, Schutz G, Yoon C, Puigserver P, Spiegelman B, Montminy M. CREB regulates hepatic gluconeogenesis through the coactivator PGC-1. *Nature* 2001;413:179-183
- Klingmuller U, Bauer A, Bohl S, Nickel PJ, Breitkopf K, Dooley S, Zellmer S, Kern C, Merfort I, Sparna T, Donauer J, Walz G, Geyer M, Kreutz C, Hermes M, Gotschel F, Hecht A, Walter D, Egger L, Neubert K, Borner C, Brulport M, Schormann W, Sauer C, Baumann F, Preiss R, MacNelly S, Godoy P, Wiercinska E, Ciucian L, Edelmann J, Zeilinger K, Heinrich M, Zanger UM, Gebhardt R, Maiwald T, Heinrich R, Timmer J, von Weizsacker F, Hengstler JG. Primary mouse hepatocytes for systems biology approaches: a standardized in vitro system for modelling of signal transduction pathways. *IEE Syst Biol* 2006;153:433-447
- Chen H, Charlat O, Tartaglia LA, Woolf EA, Weng X, Ellis SJ, Lakey ND, Culpepper J, Moore KJ, Breitbart RE, Duyk GM, Tepper RI, Morgenstern JP. Evidence that the diabetes gene encodes the leptin receptor: identification of a mutation in the leptin receptor gene in db/db mice. *Cell* 1996;84:491-495
- Rigotti A, Trigatti BL, Penman M, Rayburn H, Herz J, Krieger M. A targeted mutation in the murine gene encoding the high density lipoprotein (HDL) receptor scavenger receptor class B type I reveals its key role in HDL metabolism. *Proc Natl Acad Sci USA* 1997;94:12610-12615
- Pelleymounter MA, Cullen MJ, Baker MB, Hecht R, Winters D, Boone T, Collins F. Effects of the obese gene product on body weight regulation in ob/ob mice. *Science* 1995;269:540-543
- Leiter EH, Reifsnyder PC. Differential levels of diabetogenic stress in two new mouse models of obesity and type 2 diabetes. *Diabetes* 2004;53(Suppl. 1):S4-S11
- Mesli S, Javorschi S, Berard AM, Landry M, Priddle H, Kivlichan D, Smith AJ, Yen FT, Bihain BE, Darmon M. Distribution of the lipolysis stimulated receptor in adult and embryonic murine tissues and lethality of LSR-/- embryos at 12.5 to 14.5 days of gestation. *Eur J Biochem* 2004;271:3103-3114
- Saad MJ, Araki E, Miralpeix M, Rothenberg PL, White MF, Kahn CR. Regulation of insulin receptor substrate-1 in liver and muscle of animal models of insulin resistance. *J Clin Invest* 1992;90:1839-1849
- Considine RV, Sinha MK, Heiman ML, Kriauciunas A, Stephens TW, Nyce MR, Ohannesian JP, Marco CC, McKee LJ, Bauer TL, Caro JF. Serum immunoreactive-leptin concentrations in normal-weight and obese humans. *N Engl J Med* 1995;334:292-295
- Halaas JL, Gajiwala KS, Maffei M, Cohen SL, Chait BT, Rabinowitz D, Lallone RL, Burley SK, Friedman JM. Weight-reducing effects of the plasma protein encoded by the obese gene. *Science* 1995;269:543-546
- Igel M, Becker W, Herberg L, Joost HG. Hyperleptinemia, leptin resistance, and polymorphic leptin receptor in the New Zealand obese mouse. *Endocrinology* 1997;138:4234-4239
- Plump AS, Smith JD, Hayek T, Aalto-Setälä K, Walsh A, Verstuyft JG, Rubin

- EM, Breslow JL. Severe hypercholesterolemia and atherosclerosis in apolipoprotein E-deficient mice created by homologous recombination in ES cells. *Cell* 1992;71:343–353
37. Silver DL, Jiang XC, Tall AR. Increased high density lipoprotein (HDL), defective hepatic catabolism of ApoA-I and ApoA-II, and decreased ApoA-I mRNA in *ob/ob* mice. Possible role of leptin in stimulation of HDL turnover. *J Biol Chem* 1999;274:4140–4146
38. Bihain BE, Yen FT. Free fatty acids activate a high-affinity saturable pathway for degradation of low-density lipoproteins in fibroblasts from a subject homozygous for familial hypercholesterolemia. *Biochemistry* 1992; 31:4628–4636
39. Yen FT, Mann CJ, Guermani LM, Hannouche NF, Hubert N, Hornick CA, Bordeau VN, Agnani G, Bihain BE. Identification of a lipolysis-stimulated receptor that is distinct from the LDL receptor and the LDL receptor-related protein. *Biochemistry* 1994;33:1172–1180
40. Ito Y, Azrolan N, O'Connell A, Walsh A, Breslow JL. Hypertriglyceridemia as a result of human apo CIII gene expression in transgenic mice. *Science* 1990;249:790–793
41. Ueda Y, Royer L, Gong E, Zhang J, Cooper PN, Francone O, Rubin EM. Lower plasma levels and accelerated clearance of high density lipoprotein (HDL) and non-HDL cholesterol in scavenger receptor class B type I transgenic mice. *J Biol Chem* 1999;274:7165–7171